Wave Domain Sound Field Interpolation Using Two Spherical Microphone Arrays

Xiaoli Tang*, Jihui (Aimee) Zhang*, David Lou Alon†, Zamir Ben-Hur†,
Prasanga Samarasinghe* and Thushara Abhayapala*
*Audio and Acoustic Signal Processing Group
The Australian National University, Canberra, Australia
†Reality Labs Research at Meta, CA 94025, USA

***Abstract*—The demand for reproducing real and immersive auditory experiences has increased since the rise of virtual reality (VR). Various types of microphone arrays, along with processing and rendering approaches, are used to capture the true sound field in order to achieve this goal. However, auditory information is often limited to the location of the recording device and does not support expanded reproduction regions. One way to treat this is to interpolate the sound field using recordings from multiple microphone arrays. In this paper, we propose a sound field interpolation approach based on plane-wave expansion in the spherical harmonic domain. The proposed method employs the ℓ_1 norm to optimally map the true sound field onto a set of virtual plane waves. Evaluation of the reproduction error and a comparison with the error obtained when employing the ℓ_2 norm and a single microphone array with the plane-wave method, suggest that the proposed method provides higher reproduction accuracy over a larger region of interest.**

***Index Terms*—Sound field interpolation/reproduction, spherical microphone array (SMA), augmented reality (AR), virtual reality (VR), plane-wave expansion**

I. Introduction

With the rise of augmented reality (AR) and virtual reality (VR), people have set ever higher expectations from the quality of the reproduction of perceptually equivalent scenes, where the auditory experience complements the visual experience [1] [2]. For example, people wish to feel fully immersed within a virtual concert or that they are actually attending a football match. In order to create such an auditory experience, the workflow often goes through the sequential procedure of capturing, processing, reproducing and binaural rendering.

Various shapes and structures of microphones are available on the market, such as the spherical microphone array (SMA) (including EigenMike [3] and Zylia [4]), the planar array [5], and arbitrary arrays like Facebook smart glasses [6]. With the increasing trend in wearable microphone arrays, there is potential to combine information from multiple recording positions in order to achieve sound field reproduction over an extended region. At present, SMAs are typically used for capturing acoustic information at higher orders [7]; however, the recordings are restricted to the array size and the number of microphones. The trade-off sets an upper limit of the truncation order (relates to the upper effective frequency of operation of a SMA), reproduction sweet-spot size and overall accuracy [8]. There are two existing categories of approaches to enlarge the reproduction sweet-spot size without sacrificing quality or incurring high cost; these are: extrapolation and interpolation. The usefulness of each method depends on the available number of resources (i.e., recording devices), as well as on the application in terms of size requirements for listener translation. When a SMA is used for recording, extrapolation methods such as SpaMoS [9] and mixed wave expansion [10] have been proposed and developed to allow for listener translation. When multiple microphone arrays are used for recording, interpolation methods such as the weighted average interpolation method [11] and the geometry-based spatial sound acquisition technique [12] can be adopted. Interpolation often results in a larger sweet-spot, good localisation and accurate spectrum reproduction [13]. However, the reproduced sound field is often confined to the boundary of the microphone grid, or requires additional localization of direct sound field components [14]. Recently, Emura has shown improved accuracy when using two SMAs with an interpolation method based on plane-wave expansion [15]. However, the method [15] operated in the frequency domain, and the evaluation was carried out at a limited number of positions on the line connecting the two SMAs, without evaluating the performance over a larger region.

In this paper, we propose a wave-domain interpolation method using a dual-SMA to reproduce the sound field over an extended sweet-spot without degrading the quality. Specifically, we create a virtual sound field by mapping the dual-SMA recordings to a dictionary of plane waves using Iteratively Reweighted Least Squares (IRLS) [16] optimisation. We evaluate the reproduction performance by computing the root-mean-square error (RMSE) between the true sound field and the reproduced sound field over a rectangular region of interest (ROI). We benchmark the proposed method with an alternative optimisation method (dual-SMAs with ℓ_2 norm) and the plane-wave method for a single SMA with ℓ_1 norm. The simulation results in both free field and and a reverberant environment indicate an advantage of the proposed method for sound field reproduction, with a larger sweet-spot and lower RMSE throughout the ROI.

II. Problem Formulation

In this section, we formulate the problem of combining the sound field recorded by two SMAs to extend the effective reproduction region beyond the spatial volume enclosed by the

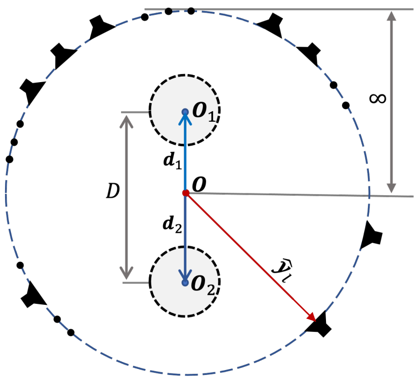

Fig. 1: Two identical SMAs set up. The equivalent virtual plane wave distribution is indicated by the surrounding loudspeakers.

two SMAs. Figure 1 illustrates a scenario with two identical SMAs separated by distance D and located at $\boldsymbol{O_1}$ and $\boldsymbol{O_2}$. The reproduced sound field is centered at the global origin $\boldsymbol{O}$. The sound field at any arbitrary point $\boldsymbol{x}$ with respect to $\boldsymbol{O}$ can be written as [17], [18]

$$P(k,\boldsymbol{x}) = \sum_{n=0}^{\infty}\sum_{m=-n}^{n} \alpha_{nm}(k)\, j_n(k|\boldsymbol{x}|)Y_{nm}(\hat{\boldsymbol{x}}), \tag{1}$$

where k is the wavenumber, $\alpha_{nm}(k)$ are the spherical harmonic coefficients, $j_n(\cdot)$ are the spherical Bessel functions of the first kind, $Y_{nm}(\cdot)$ are the spherical harmonic basis functions and $\hat{\boldsymbol{x}}$ denotes the direction of the position $\boldsymbol{x}$.

Let $\alpha_{nm}^{(1)}(k)$ and $\alpha_{nm}^{(2)}(k)$ be the spherical harmonic coefficients of the sound field with respect to the two origins of the SMAs, $\boldsymbol{O_1}$ and $\boldsymbol{O_2}$, respectively. Then, the sound field recorded by each SMA is given by

$$P^{(t)}(k,\boldsymbol{x}^{(t)}) = \sum_{n=0}^{N_t}\sum_{m=-n}^{n} \alpha_{nm}^{(t)}(k) j_n(k|\boldsymbol{x}^{(t)}|)Y_{nm}(\hat{\boldsymbol{x}}^{(t)}), \tag{2}$$

where $t \in \{1,2\}$, $\boldsymbol{x}^{(t)}$ is a point within the space occupied by the t^{th} SMA and N_t is the truncation order[1] of the SMAs. For simplicity, we consider two open SMAs in this paper. However, it is possible to incorporate the scattering effects between two rigid SMAs with the MS-HOA encoding model proposed by Kaneko [20].

The problem we address in this paper is that given the recorded spherical harmonic coefficients, $\alpha_{nm}^{(t)}(k)$, for $n = 0,\ldots,N_t$, $m = -n,\ldots,n$ and $t \in \{1,2\}$, how do we reconstruct the sound field $P(k,\boldsymbol{x})$ in (1) at $\boldsymbol{x}$ covering an extended region beyond the volumes occupied by the two recording SMAs.

III. Plane-wave Expansion of a Sound Field

We propose to solve the above problem by exploiting the plane-wave expansion method [21], [22], and therefore, in this section, we provide a brief overview of the method. The underlying concept is that any arbitrary sound field can be equivalently expressed by a superposition of many virtual plane waves. Therefore, based on this method, the sound pressure at any arbitrary position $\boldsymbol{x}$ with respect to $\boldsymbol{O}$ can be expressed by the superposition of infinitely many plane waves of

$$P(k,\boldsymbol{x}) = \int_{\hat{\boldsymbol{y}}} \psi(k,\hat{\boldsymbol{y}};\boldsymbol{O})\, e^{ik\hat{\boldsymbol{y}}\cdot\boldsymbol{x}}\, d\hat{\boldsymbol{y}}, \tag{3}$$

where $\psi(k,\hat{\boldsymbol{y}};\boldsymbol{O})$ denotes the signal received at the point $\boldsymbol{O}$ due to a plane wave at wavenumber k arriving from the direction $\hat{\boldsymbol{y}}$. Note that the literature refers to $\psi(k,\hat{\boldsymbol{y}};\boldsymbol{O})$ as the plane wave aperture function or plane wave distribution function.

Since $\psi(k,\hat{\boldsymbol{y}};\boldsymbol{O})$ is a spherical function of angles, we can decompose it into spherical harmonics by

$$\psi(k,\hat{\boldsymbol{y}};\boldsymbol{O}) = \sum_{n=0}^{\infty}\sum_{m=-n}^{n} \beta_{nm}(k)Y_{nm}(\hat{\boldsymbol{y}}), \tag{4}$$

where $\beta_{nm}(k)$ denotes the spherical harmonic coefficients of $\psi(k,\hat{\boldsymbol{y}};\boldsymbol{O})$. By substituting (4) and the spherical harmonic expansion of $e^{ik\hat{\boldsymbol{y}}\cdot\boldsymbol{x}}$ into (3), we obtain the plane-wave expansion of the sound field as

$$P(k,\boldsymbol{x}) = \sum_{n=0}^{\infty}\sum_{m=-n}^{n} 4\pi i^n \beta_{nm}(k) j_n(k|\boldsymbol{x}|)Y_{nm}(\hat{\boldsymbol{x}}). \tag{5}$$

By equating (1) and (5), we express the plane wave distribution coefficients in terms of wave field coefficients as

$$\beta_{nm}(k) = \frac{(-i)^n}{4\pi}\alpha_{nm}(k). \tag{6}$$

IV. Combining dual spherical microphone arrays via plane-wave expansion

In this section, we apply the plane-wave expansion to propose a method for dual-SMA sound field interpolation.

A. SMA coefficients in terms of plane wave distribution

Since the received signals due to a plane wave at two different points are related by a simple phase difference (time delay) [23], the plane wave distribution as seen by $\boldsymbol{O}_t$ is given by

$$\psi(k,\hat{\boldsymbol{y}};\boldsymbol{O}_t) = e^{-ik\hat{\boldsymbol{y}}_l\cdot\boldsymbol{d}_t}\, \psi(k,\hat{\boldsymbol{y}}_l;\boldsymbol{O}), \tag{7}$$

where $\boldsymbol{d}_t$ is a vector towards the point $\boldsymbol{O}_t$ from $\boldsymbol{O}$.

Using (4), (6) and (7), we express the sound field coefficients measured by the SMA at $\boldsymbol{O}_t$ as

$$\begin{aligned}\alpha_{nm}^{(t)}(k) &= \int_{\hat{\boldsymbol{y}}} 4\pi i^n\, Y_{nm}^{*}(\hat{\boldsymbol{y}})\, e^{ik\hat{\boldsymbol{y}}\cdot\boldsymbol{d}_t}\psi(k,\hat{\boldsymbol{y}};\boldsymbol{O})d\hat{\boldsymbol{y}} \\ &\approx \sum_{l=1}^{L} 4\pi i^n\, Y_{nm}^{*}(\hat{\boldsymbol{y}}_l)\, e^{ik\hat{\boldsymbol{y}}_l\cdot\boldsymbol{d}_t}\psi(k,\hat{\boldsymbol{y}}_l;\boldsymbol{O}),\end{aligned} \tag{8}$$

[1]Note that for a 32-channel EigenMike, the maximum N_t is 4 [19] and also N_t is a function of frequency/wavenumber k.

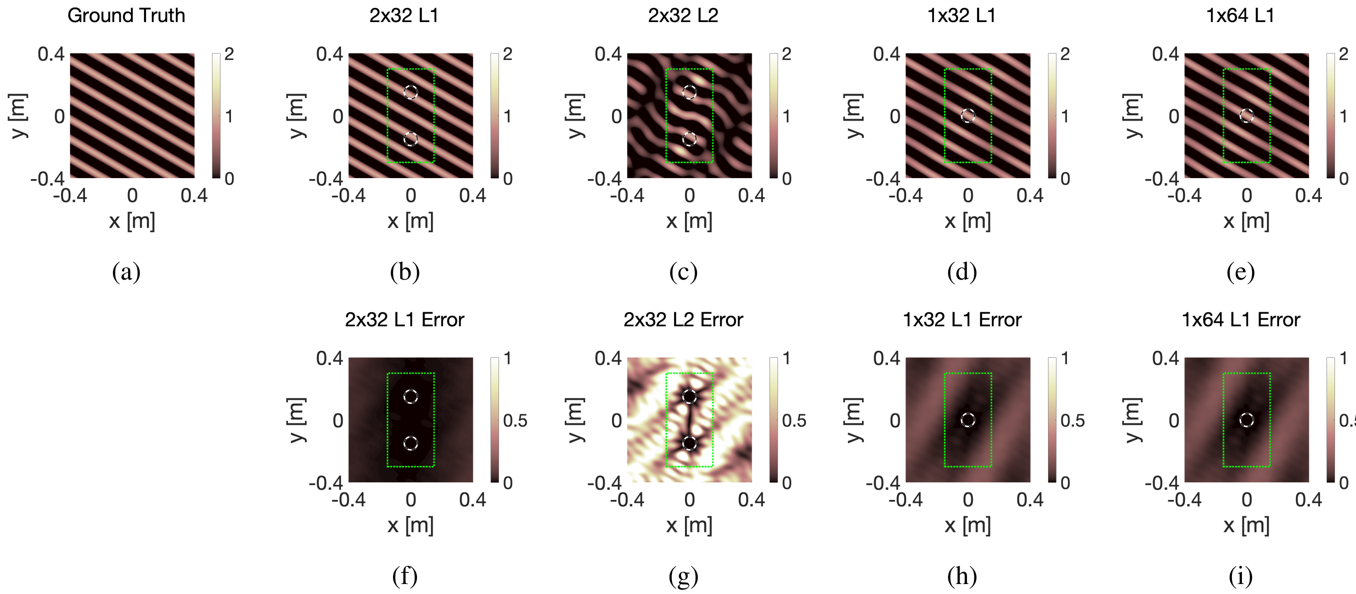

Fig. 2: Comparison in free field of the true sound field (a), the reproduced sound field using the proposed method (b), the benchmarks (c) - (e), and the corresponding reproduction error in the horizontal plane (no elevation) (f) - (i), for a single sound source at 3125 Hz. The dotted circles denote the two SMAs, and the green rectangle denotes our ROI with width 0.3 m and length 0.6 m, and the separation distance D was 0.3 m.

where we approximate the plane wave aperture function by a discrete number of plane waves, L. We use this finite number of plane waves as a dictionary set in the following section.

B. Dual-SMA Interpolation

We use (8) with $t = 1$ and 2 to write the matrix equation

$$\begin{bmatrix} \boldsymbol{A}^{(1)} \\ \boldsymbol{A}^{(2)} \end{bmatrix} \boldsymbol{\psi_O} = \begin{bmatrix} \boldsymbol{\alpha}^{(1)} \\ \boldsymbol{\alpha}^{(2)} \end{bmatrix}, \tag{9}$$

where $\boldsymbol{A}^{(t)}$ is a $(N_t{+}1)^2{\times}L$ matrix with $(n^2{+}n{+}m{+}1, l^{\text{th}})$ elements given by $\boldsymbol{A}^{(t)}(nm,l) = 4\pi(i)^n Y^*_{nm}(\hat{\boldsymbol{y}}_l)e^{ik\hat{\boldsymbol{y}}_l \boldsymbol{d}_t}$, $\boldsymbol{\alpha}^{(t)}{=}[\alpha^{(t)}_{00},\ldots,\alpha^{(t)}_{N_tN_t}]^T$ and $\boldsymbol{\psi}_O{=}[\psi(\hat{\boldsymbol{y}}_1;\boldsymbol{O}),\ldots,\psi(\hat{\boldsymbol{y}}_L;\boldsymbol{O})]^T$.

We formulate (9) as an optimisation problem to solve for an optimal set of plane waves $\boldsymbol{\psi}_O$ as

$$\min \|\boldsymbol{e}\|_p \qquad \text{subject to} \;\; \boldsymbol{e} = \boldsymbol{A}\boldsymbol{\psi_O} - \boldsymbol{\alpha}, \tag{10}$$

where $\boldsymbol{A} = [\boldsymbol{A}^{(1)}, \boldsymbol{A}^{(2)}]^T$, $\boldsymbol{\alpha} = [\boldsymbol{\alpha}^{(1)}, \boldsymbol{\alpha}^{(2)}]^2$, and $\|\cdot\|_p$ denotes the p-norm. The least squares (ℓ_2) solution is given by $\boldsymbol{\psi_O}{=}\boldsymbol{A}^\dagger\boldsymbol{\alpha}$ where $(\cdot)^\dagger$ denotes the Moore-Penrose inverse [24].

One of the approaches is to use the Iteratively Re-weighted Least Squares (IRLS) method to minimise error $\boldsymbol{e}$ in (10) in the ℓ_1 sense. Using the derivation in [16], we iteratively solve for $\boldsymbol{\psi_O}$ by

$$\boldsymbol{\psi_O} = \left(\boldsymbol{A^T W^T W A}\right)^{-1} \boldsymbol{A^T W^T W \alpha}, \tag{11}$$

where $\boldsymbol{W}$ is a diagonal matrix of the error weights, starting with unity weighting $\boldsymbol{W}{=}\boldsymbol{I}$ to solve for the initial state of $\boldsymbol{\psi_O}$. We update $\boldsymbol{W}$ at each iteration to obtain the optimal set of $\boldsymbol{\psi_O}$.

V. SIMULATION AND EVALUATIONS

In this section, we evaluate the performance of the proposed method based on a detailed simulation study.

A. Simulation Setup

The performance evaluation is carried out in both free-field (using Green's function) and reverberant environments (using the Image Source Method [25]). A single true sound source is used in both scenarios. In the reverberant environment case, the room size is $(4, 5, 2.5)$ m, the reverberation time is $T_{60}{=}0.3$ s, and the single true sound source is positioned inside the room at $(1, 1.73, 0)$ m in Cartesian coordinates as a point source. The two SMAs mimic EigenMike geometry [26] with 32 microphones and a radius of 0.042 m. For comparison, we use the benchmark of having only one SMA at origin, consisting of either 32 microphones or 64 microphones (in this case, the microphone positions follow the Fliege distribution [27]). We select the single SMA scenario as the benchmark to demonstrate the translation performance based on the number of resources available (one vs two devices/SMAs). Note that all SMAs used in this study are assumed to be open spheres.

B. Simulation Results

Figure 2 shows an example comparison of reproduced sound fields and reproduction error. Sound field reproduction is compared between four methods: a single 32-channel SMA with ℓ_1 norm, a single 64-channel SMA with ℓ_1 norm, and two 32-channel SMAs with ℓ_1 and ℓ_2 norms. For the single SMA scenarios, the center of the SMA overlaps with the global origin $\boldsymbol{O}$. The proposed method in Figure 2 (b) (f) shows superiority in terms of low reproduction error compared

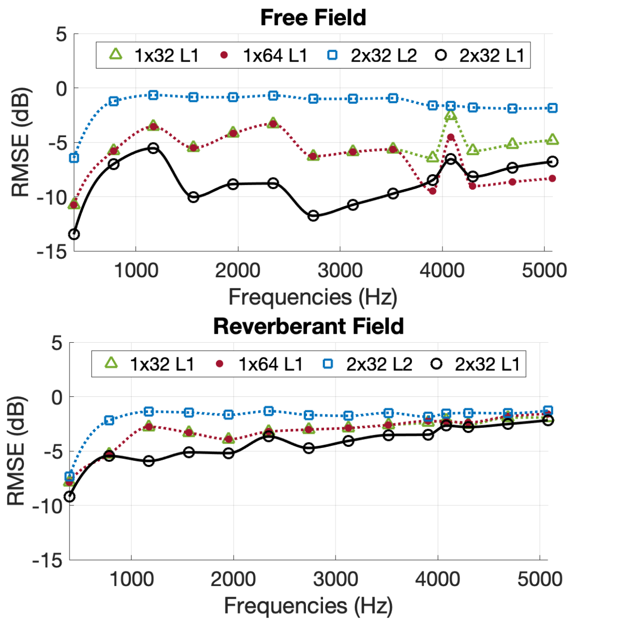

Fig. 3: RMSE comparison between reproduction methods (single and dual SMAs, ℓ_2 and ℓ_1 norm optimisations) at different frequencies in the range $(0, 5200)$ Hz. The separation distance between two SMA centers is $D = 0.3$ m.

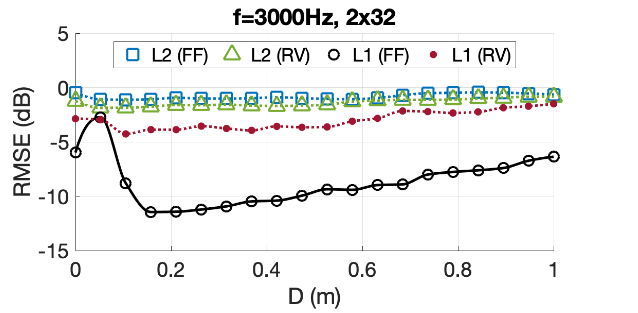

Fig. 4: RMSE comparison in free field and reverberation environment with ℓ_2 and ℓ_1 optimisations versus the separation distance D between two SMA centers. The ROI is with width 0.3 m and length 0.6 m. The true sound field frequency is 3000 Hz.

with the benchmarks in free field. A larger area with a consistently low reproduction error can be observed in the proposed method.

We evaluate the performance of the proposed interpolation method by computing RMSE between the reproduced sound field and the true sound field, given by

$$RMSE_{dB} = 10 \log_{10} \sqrt{\frac{1}{q} \sum_{i=1}^{q} (P_i^{\text{rep}} - P_i^{\text{true}})^2}, \tag{12}$$

where q is the number of observation points inside the ROI (a rectangular region on the horizontal plane spanned by the centres of the two recording SMAs, with a dimension of 0.3 m by 0.6 m), and P_i^{rep} and P_i^{true} denote the reproduced sound pressure and true sound pressure at the i^{th} observation point, obtained from (3).

In Figure 3, a similar comparison at different frequencies is presented. The frequency range is truncated to a maximum of 5200 Hz due to the limited order (accurate up to the 4^{th}) of this specific size and configuration of SMAs. For both the free field and the reverberant scenarios, the lowest error can be observed from the proposed method of two SMAs with IRLS throughout most frequencies, with RMSE approximately -10 dB and -5 dB, respectively. Above 4000 Hz, the advantage over a single 64-channel SMA is not obvious. The spikes at around 4083 Hz indicate inaccurate recording due to the spherical Bessel functions division by zero problem [28], which can be overcome by using rigid-sphere SMAs. While not presented here, we also simulated a single 64-channel SMA with double the radius, and the RMSE turned out to be lower than with the proposed method. However, since the size of the ROI covered by this SMA was doubled, we considered the comparison to be not be fair in this context.

Note that the weak results from ℓ_2 interpolation are caused by the sparse nature of the single true sound source. In contrast, the proposed method shows little advantage in reverberant environments because the sound field now has multiple sound reflections and is no longer sparse. Another reason for worse performance under reverberation is the difficulty of reproducing near-field sources with only plane waves.

Figure 4 illustrates the performance against varying SMA separation distance D while keeping the ROI size fixed. With ℓ_1 norm optimisation, the reproduction error is observed to be large when the two SMAs are partially overlapped. Once the two SMAs are apart, the RMSE firstly drops and then increases as D increases due to less information inside ROI having been captured by the SMAs.

VI. CONCLUSION

We propose a novel method for sound field reproduction using recordings from two SMAs. By interpolating the sound field and mapping to a set of virtual plane waves, the sound field reproduction region can be enlarged and the accuracy can be improved. The method was validated through simulation on open-sphere SMAs and benchmarked against conventional methods. We also observed a relationship between the separation distance between the SMAs and the reproduction performance, which should be further investigated in order to achieve optimised geometrical positioning. However, the proposed method showed less advantage in a reverberant environment. This can be overcome by extending the plane-wave to a mixed-wave method including both virtual point sources and plane wave sources. Plane-wave distribution is the starting point to validate this idea, and we will explore other approaches in the next stage of future work. Future research also includes adding mutual scattering to the SMA recordings and carrying out binaural rendering and perceptual tests.

REFERENCES

[1] R. Graham and S. Cluett, "The Soundfield as Sound Object: Virtual Reality Environments as a Three-Dimensional Canvas for Music Composition," in *Proc. Audio Eng. Soc. Int. Conf.*, Sept. 2016, pp. 3–7.

[2] P. Dodds, S. V. A. Garí, W. O. Brimijoin and P. W. Nov, Robinson, "Auralization systems for simulation of augmented reality experiences in virtual environments," in *Proc. ICSA 5th Int. Conf.*, Nov. 2019, p. 4.

[3] Eigenmike, "Eigenmike microphone." mhacoustics.com https://mhacoustics.com/products (accessed Aug. 08, 2021).

[4] E. Patricio, M. Skrok, and T. Zernicki, "Recording and Mixing of Classical Music Using Non-Adjacent Spherical Microphone Arrays and Audio Source Separation Algorithms," in *Conv. 147th Audio Eng. Soc.*, 2019.

[5] H. Chen, T. D. Abhayapala, and W. Zhang, "Theory and design of compact HYBRID microphone arrays on two-dimensional planes for three-dimensional soundfield analysis," in *The J. of the ASA*, vol. 138, no. 5, pp. 3081–3092, 2015.

[6] Facebook, "Ray-Ban and Facebook introduce Ray-Ban Stories, first-generation smart glasses." tech.fb.com. https://tech.fb.com/ray-ban-and-facebook-introduce-ray-ban-stories-first-generation-smart-glasses/ (accessed Sept. 12, 2021).

[7] B. Rafaely, "Analysis and design of spherical microphone arrays," in *IEEE Transactions on Speech and Audio Processing*, vol. 13, no. 1, pp. 135-143, Jan. 2005.

[8] P. Samarasinghe, "Modal based solutions for the acquisition and rendering of large spatial soundfields," Ph.D. dissertation, Dept. Eng., Australian National Univ., Canberra, ACT, Australia, 2015.

[9] T. Pihlajamäki, and V. Pulkki, "Projecting Simulated or Recorded Spatial Sound onto 3D-Surfaces," in *Proc. Audio Eng. Soc. Int. Conf.*, Mar. 2012, pp. 4-5.

[10] L. Birnie, T. Abhayapala, P. Samarasinghe and V. Tourbabin, "Sound Field Translation Methods for Binaural Reproduction," *2019 IEEE Workshop on WASPAA*, 2019, pp. 140-144.

[11] A. Southern, J. Wells and D. Murphy, "Rendering walk-through auralisations using wave-based acoustical models," *2009 17th European Signal Processing Conf.*, 2009, pp. 715-719.

[12] O. Thiergart, G. Del Galdo, M. Taseska and E. A. P. Habets, "Geometry-Based Spatial Sound Acquisition Using Distributed Microphone Arrays," in *IEEE Transactions on Audio, Speech, and Language Processing*, vol. 21, no. 12, pp. 2583-2594, Dec. 2013.

[13] J. G. Tylka and E. Y. Choueiri, "Fundamentals of a parametric method for virtual navigation within an array of ambisonics microphones," *J. Audio Eng. Soc.*, vol. 68, no. 3, pp. 120–137, 2020.

[14] L. Birnie, T. Abhayapala, V. Tourbabin and P. Samarasinghe, "Mixed Source Sound Field Translation for Virtual Binaural Application With Perceptual Validation," in *IEEE/ACM Transactions on Audio, Speech, and Language Processing*, vol. 29, pp. 1188-1203, 2021.

[15] S. Emura, "Sound field estimation using two spherical microphone arrays," *2017 IEEE International Conference on Acoustics, Speech and Signal Processing (ICASSP)*, 2017, pp. 101-105.

[16] C. S. Burrus, "Vector Space and Matrix Methods in Signal and System Theory" in *arXiv: Signal Processing*, pp. 1-45, 2019.

[17] B. Rafaely, *Fundamentals of Spherical Array Processing*. Berlin, Heidelberg: Springer Berlin Heidelberg, 2015.

[18] T. D. Abhayapala and D. B. Ward, "Theory and design of high order sound field microphones using spherical microphone array," in *IEEE Int. Conf. on Acoustics, Speech, and Signal Processing*, May 2002, pp. 1949-1952.

[19] S. Brown and D. Sen, "Error analysis of spherical harmonic soundfield representations in terms of truncation and aliasing errors," in *2013 IEEE International Conference on Acoustics, Speech and Signal Processing*, 2013, pp. 360-364.

[20] S. Kaneko and R. Duraiswami, "Multiple scattering ambisonics: three-dimensional sound field estimation using Interacting spheres," in *JASA Express Letters*, vol. 1, no. 8, pp. 1–11, Aug. 2021.

[21] M. Park and B. Rafaely, "Sound-field analysis by plane-wave decomposition using spherical microphone array," in *The J. of the ASA*, vol. 118, pp. 3094-3103, 2005.

[22] L. S. Davis, R. Duraiswami, E. Grassi, N. A. Gumerov, Z. Li, and D. N. Zotkin, "High Order Spatial Audio Capture and Its Binaural Head-Tracked Playback Over Headphones with HRTF Cues," in *Conv. 119th Audio Eng. Soc.* Paper 6540, Oct. 2005.

[23] D. Menzies and M. Al-Akaidi, "Nearfield binaural synthesis and ambisonics," *J. Acoust. Soc. Amer.,* vol. 121, no. 3, pp. 1559-1563, 2007.

[24] C. C. Pugh, *Real Mathematical Analysis*, 2nd ed. Springer, 2015.

[25] R. A. Rathnayake and W. K. I. L. Wanniarachchi, "Image Source Method Based Acoustic Simulation For 3-D Room Environment," in *Int. J. of Scientific & Tech. Res.*, vol. 8, no. 11, pp. 222-228, Nov. 2019.

[26] *em32 Eigenmike® microphone array release notes (v15.0)*, Mhacoustics Co., New Jersey, NJ, USA, 2013. [Online]. Available: https://mhacoustics.com/sites/default/files/EigenmikeReleaseNotesV15.pdf

[27] J. Fliege and U. Maier, "The distribution of points on the sphere and corresponding cubature formulae," in *IMA J. of Numerical Analysis*, vol. 19, no. 2, pp. 317-334, April 1999.

[28] S. Moreau, J. Daniel and S. Bertet, "3D Sound Field Recording with Higher Order Ambisonics – Objective Measurements and Validation of a 4^{th} Order Spherical Microphone," in *Proc. Audio Eng. Soc. Int. Conf.*, May 2006, pp. 6857-6881.

[29] P. Series, "Methods for objective and subjective assessment of speech and video quality", *International Telecommunication Union Radiocommunication Assembly*, 2016.